Journal of Zhejiang University-SCIENCE B (Biomedicine & Biotechnology) 2024 25(6):485-498
www.jzus.zju.edu.cn; www.springer.com/journal/11585
E-mail: jzus_b@zju.edu.cn

Research Article

https://doi.org/10.1631/jzus.B2300917

Sialyltransferase ST3GAL6 silencing reduces α2,3-sialylated glycans to regulate autophagy by decreasing HSPB8-BAG3 in the brain with hepatic encephalopathy

Xiaocheng LI[1], Yaqing XIAO[1], Pengfei LI[3], Yayun ZHU[1], Yonghong GUO[4]✉, Huijie BIAN[2]✉, Zheng LI[1]✉

[1]*Laboratory for Functional Glycomics, College of Life Sciences, Northwest University, Xi'an 710069, China*
[2]*National Translational Science Center for Molecular Medicine, Department of Cell Biology, Fourth Military Medical University, Xi'an 710032, China*
[3]*Medical Experiment Center, Shaanxi University of Chinese Medicine, Xianyang 712046, China*
[4]*The Infectious Disease Department, Gongli Hospital, Pudong New Area, Shanghai 200135, China*

Abstract: End-stage liver diseases, such as cirrhosis and liver cancer caused by hepatitis B, are often combined with hepatic encephalopathy (HE); ammonia poisoning is posited as one of its main pathogenesis mechanisms. Ammonia is closely related to autophagy, but the molecular mechanism of ammonia's regulatory effect on autophagy in HE remains unclear. Sialylation is an essential form of glycosylation. In the nervous system, abnormal sialylation affects various physiological processes, such as neural development and synapse formation. ST3 β-galactoside α2,3-sialyltransferase 6 (ST3GAL6) is one of the significant glycosyltransferases responsible for adding α2,3-linked sialic acid to substrates and generating glycan structures. We found that the expression of ST3GAL6 was upregulated in the brains of mice with HE and in astrocytes after ammonia induction, and the expression levels of α2,3-sialylated glycans and autophagy-related proteins microtubule-associated protein light chain 3 (LC3) and Beclin-1 were upregulated in ammonia-induced astrocytes. These findings suggest that ST3GAL6 is related to autophagy in HE. Therefore, we aimed to determine the regulatory relationship between ST3GAL6 and autophagy. We found that silencing ST3GAL6 and blocking or degrading α2,3-sialylated glycans by way of *Maackia amurensis* lectin-II (MAL-II) and neuraminidase can inhibit autophagy. In addition, silencing the expression of ST3GAL6 can downregulate the expression of heat shock protein β8 (HSPB8) and Bcl2-associated athanogene 3 (BAG3). Notably, the overexpression of HSPB8 partially restored the reduced autophagy levels caused by silencing ST3GAL6 expression. Our results indicate that ST3GAL6 regulates autophagy through the HSPB8-BAG3 complex.

Key words: Hepatic encephalopathy; Hyperammonemia; Autophagy; ST3 β-galactoside α2,3-sialyltransferase 6 (ST3GAL6); Heat shock protein β8 (HSPB8)

1 Introduction

Hepatic encephalopathy (HE) is a common complication of acute and chronic liver dysfunction. HE is mainly characterized by metabolic disorders and neuropsychiatric abnormalities, including the impairment of motor, sensory, and cognitive functions at varying severities (Rose et al., 2020); neuroinflammation and neuronal cell death are its main pathological features (Ochoa-Sanchez et al., 2021). The pathogenesis of HE is complex and remains to be fully understood. However, among the many proposed pathogenesis mechanisms, the ammonia poisoning theory is often generally accepted (Fallahzadeh and Rahimi, 2022). This theory suggests that impaired liver function leads to impaired ammonia clearance and increased blood ammonia; the elevated blood ammonia enters the brain through the blood–brain barrier, interfering with the function and metabolism of brain cells, especially astrocytes, ultimately causing brain cell edema and oxidative stress, triggering

✉ Zheng LI, zhengli@nwu.edu.cn
Huijie BIAN, hjbian@fmmu.edu.cn
Yonghong GUO, gyh01678@glhospital.com
Zheng LI, https://orcid.org/0000-0002-1839-3450
Huijie BIAN, https://orcid.org/0000-0003-4690-4622
Yonghong GUO, https://orcid.org/0000-0001-8076-1018

Received Dec. 17, 2023; Revision accepted Feb. 20, 2024;
Crosschecked Apr. 23, 2024; Published online May 15, 2024

a series of neurological symptoms (Sepehrinezhad et al., 2020).

Sialylation is one of the most common glycosylation processes, which covalently adds sialic acid to the termini of glycoconjugates. Sialylation is a biochemically substantial modification in various cellular functions, such as cell adhesion and signal transduction (Huang et al., 2022). Sialyltransferase (ST) includes 20 members and is divided into four subfamilies: ST3 β-galactoside α2,3-sialyltransferases 1–6 (ST3GAL1–6; α2,3 link type), ST6 β-galactoside α2,6-sialyltransferases 1 and 2 (ST6GAL1–2; α2,6 link type), ST6 *N*-acetylgalactosaminide α2,6-sialyltransferases 1–6 (ST6GALNAc1–6; α2,6 link type), and ST8 α-*N*-acetylneuraminide α2,8-sialyltransferases 1–6 (ST8SIA1–6; α2,8 link type) (Bowles and Gloster, 2021). These sialyltransferases are responsible for the transfer of sialic acid and participate in post-translational modification of proteins. Many studies have shown that abnormal sialyltransferase expression levels are closely related to the occurrence and development of various diseases, such as neurodegeneration, tumors, and immune system diseases (Kim, 2020). ST3GAL6 is one of the main enzymes responsible for forming α2,3-sialylated *N*-glycans or *O*-glycans. Most reports on ST3GAL6 focus on tumor research, for example, in bladder cancer and lung adenocarcinoma (Dalangood et al., 2020; Li et al., 2022). In addition, studies have pointed out that *ST3GAL6* mutations exist in the neurodegenerative disease amyotrophic lateral sclerosis (ALS) (Togawa et al., 2019). However, the exact regulatory function and mechanism of ST3GAL6 remain a mystery in the disease, despite it being an essential glycosyltransferase for α2,3-sialylation.

Autophagy refers to the lysosomal degradation of damaged or excess components; as an evolutionarily conserved mechanism in eukaryotes, autophagy can help cells counteract different intracellular and extracellular stress signals and is essential for maintaining cellular homeostasis. In mammals, nervous system cells are particularly susceptible to damage, and the functional integrity of cells and tissues depends largely on removing damaged organelles and defective proteins to prevent the accumulation of neurotoxicity (Friedman, 2011). Autophagy is a stress response to misfolded proteins, damaged organelles, and insoluble protein aggregates, and its damage and defects are closely related to neurological diseases (Peker and Gozuacik, 2020). Many studies have pointed out that autophagy and lysosomal systems are abnormal in neurodegenerative diseases, including Alzheimer's disease (AD), tauopathies, and Huntington's disease (HD) (Filippone et al., 2022). Ammonia is a highly diffusible weak base that can pass through the blood–brain barrier; current research shows that ammonia has a dual effect on autophagy. At high concentrations, it will damage lysosomal function and lead to defects in the degradation of autophagy substrates. At low concentrations, ammonia will activate autophagy (Soria and Brunetti-Pierri, 2019). Astrocytes are critical for detoxifying ammonia in the brain, and impaired astrocyte function is thought to be a significant cause of neuronal damage and eventual cognitive and motor symptoms in HE (Sepehrinezhad et al., 2020; Lawrence et al., 2023). Although autophagy is closely related to neurological diseases, there are few reports on whether autophagy is altered in astrocytes and the brain during hyperammonemia.

In the present study, the central objective is to explore the differential expression patterns of ST3GAL6 in hepatitis B virus (HBV) transgenic mice and ammonia-induced astrocytes. Our research strives to deepen the understanding of the regulatory connection between ST3GAL6 and autophagy by assessing shifts in autophagic activity following the targeted silencing of ST3GAL6 in ammonia-induced astrocytes. Furthermore, we aim to concurrently silence ST3GAL6 expression and induce heat shock protein β8 (HSPB8) overexpression within these cells. This dual intervention aims to provide insights into the complex regulatory triad comprising ST3GAL6, HSPB8, and autophagy under ammonia induction.

2 Materials and methods

2.1 Animal model

HBV transgenic mice C57BL/6J-TG (ALB1HBV) 44BRI/J and negative control C57BL/6 mice were obtained from VITALRIVER (Beijing, China). HBV transgenic mouse and C57BL/6 mouse colonies were maintained at the Cell Engineering Research Centre and Department of Cell Biology of Fourth Military Medical University (Xi'an, China). The experimental protocol involved used HBV transgenic mice (n=6) and C57BL/6 mice (n=6) as study subjects.

2.2 Cell culture and treatments

Human brain astrocyte (SVGp12) cells were kindly donated by the Cell Engineering Research Centre and Department of Cell Biology of the Fourth Military Medical University (Xi'an, China). SVGp12 cells were cultured in Dulbecco's modified Eagle's medium (DMEM; Hyclone, USA) supplemented with 10% (volume fraction) fetal bovine serum (FBS; Invitrogen, USA) and 1% (volume fraction) penicillin/streptomycin (ThermoFisher, USA) in an incubator with 5% CO_2 at 37 ℃. Bafilomycin A1 (Baf A1; 5084090001), neuraminidase (derived from *Clostridium perfringens*, N2876), and NH_4Cl (213330) were obtained from Sigma-Aldrich (USA). *Maackia amurensis* lectin-II (MAL-II; L-1260) was purchased from Vector Laboratories (USA). To achieve HSPB8 overexpression, we inserted the homo sapiens full open reading frame complementary DNA (cDNA) clone of HSPB8 into a pcDNA3.1 vector. Plasmid propagation during plasmid construction was carried out using *Escherichia coli* DH5α, and plasmid construction was completed by the Transheep Bio Company (Shanghai, China). Small interfering RNAs (siRNAs) of ST3GAL6 were designed and synthesized by Transheep Bio Company. SVGp12 cells were transfected with the overexpression plasmid and siRNAs using the Lipo3000 transfection reagent (Invitrogen). The specific siRNA sequences of ST3GAL6 are provided in Table S1.

2.3 Lectin microarrays

The proteins were labeled with Cy3 fluorescent dye (GE Healthcare, USA) and purified using Sephadex G-25 columns (GE Healthcare). Lectins were purchased from Sigma or Vector laboratories. Epoxy silane-coated glass slides were employed to establish an array encompassing 37 lectin spots, each targeting distinct glycans. The slides were exposed to a diluted solution of Cy3-labeled proteins in an incubation buffer and were allowed to incubate at room temperature for 3 h. Microarrays were scanned utilizing a GenePix 4000B confocal scanner (Axon Instruments, USA). The resultant images were analyzed for Cy3 signal detection employing GenePix 3.0 software. The experimental group's normalized fluorescence intensity (NFI) was juxtaposed with that of the control group. Fold change of >1.50 or <0.67 in pairs indicated upregulation or downregulation, respectively. *P* values of less than 0.05 were considered statistically significant.

2.4 Western blotting analysis

The total protein (30 μg) from mouse brain tissue or cell samples was separated on 8%–12% (1%= 0.01 g/mL) sodium dodecyl sulfate (SDS) gels and transferred onto polyvinylidene difluoride (PVDF) membranes. The signals were visualized using western enhanced chemiluminescence (ECL) blotting substrate (Bio-Rad, Hercules, USA) and imaged with the Qinxiang imaging system (Qinxiang, Shanghai, China). The primary antibodies used in the experiment were as follows: microtubule-associated protein light chain 3B (LC3B; 1:1000 (volume ratio, the same below), 14600-1-AP), glyceraldehyde-3-phosphate dehydrogenase (GAPDH; 1:5000, 10494-1-AP), ST3GAL6 (1:1000, 13154-1-AP), HSPB8 (1:1000, 15287-1-AP), Bcl2-associated athanogene 3 (BAG3; 1:3000, 10599-1-AP) (ProteinTech Group, IL, USA), and Beclin-1 (1:1000, 381896) (ZEN Bio, Chengdu, China). The secondary antibody was goat rabbit-horseradish peroxidase (HRP) (1:5000, 170-6515) (Bio-Rad).

2.5 Fluorescence-based lectin cytochemistry

Labeled with Cy5 fluorescent dye (GE Healthcare) and purified using a Sephadex G-25 column (GE Healthcare), cells were incubated with Cy5-labeled lectin MAL-II overnight at 4 ℃, and then stained with 1 μg/mL 4',6-diamidino-2-phenylindole (DAPI) for 10 min. Images were acquired using a laser scanning confocal microscope SP8X (Leica, Wetzlar, Germany).

2.6 Green fluorescent protein (GFP)-LC3 expression analysis

Before treatment, cells within each experimental group were transduced with GFP-LC3 adenovirus (Beyotime, Shanghai, China). Subsequently, the cells from each group were fixed using 4% (0.04 g/mL) paraformaldehyde for 30 min, followed by nuclear staining with DAPI. An SP8X laser scanning confocal microscope was utilized to capture the images.

2.7 Statistical analyses

Numerical data are shown as mean±standard deviation. Student's *t*-test was used when comparing two groups, and multivariate analysis of variance (ANOVA) was used when comparing more than two groups. A *P* value of 0.05 was considered statistically significant. Statistical analysis was performed using GraphPad Prism (GraphPad Software Inc., CA, USA).

3 Results

3.1 Effects of ammonia on ST3GAL6 and α2,3-sialylated glycans in astrocytes

To analyze the association between ammonia induction and ST3GAL6 and α2,3-sialylated glycans in astrocytes, we first used immunoblotting to detect the expression of ST3GAL6 in the brain tissues of HBV transgenic mice C57BL/6J-TG (ALB1HBV) 44BRI/J (n=6, the same age) and performed a negative control with C57BL/6 mice (n=6, the same age). The results showed that ST3GAL6 expression was upregulated in the three time periods of 8, 12, and 16 months (Figs. 1a and 1b). Subsequently, we used NH_4Cl to induce astrocytes (SVGp12) to simulate hyperammonemia in vitro. After 24 h without serum, astrocytes were treated with 2, 5, or 10 mmol/L NH_4Cl for 72 h, and the medium was changed daily to maintain the concentration of NH_4Cl. Western blotting results showed that the expression of ST3GAL6 was upregulated when stimulated by 2 mmol/L NH_4Cl (Figs. 1c and 1d). At the same time, we used lectin microarrays, consisting of 37 lectin probes, to detect changes of protein glycopatterns in SVGp12 cells induced by different concentrations of ammonia. The layout of the lectin microarray was shown in Fig. S1. Notably, the NFI of MAL-II that recognized the Siaα2-3Gal structure had a significant increase in SVGp12 cells with NH_4Cl (2 mmol/L) treatment, which was consistent with the observed upregulated expression of ST3GAL6 in SVGp12 cells (Figs. 1e and 1f). Using fluorescence-based lectin cytochemistry, we verified the expression distribution of α2,3-sialylated glycans in NH_4Cl-treated astrocytes. The fluorescence intensity can reflect the binding amount of the MAL-II to α2,3-sialylated glycan structure to indicate its expression level. This observation was consistent with results in lectin microarrays; the expression of α2,3-sialylated glycans recognized by MAL-II was significantly increased in the NH_4Cl (2 mmol/L)-treated group compared with the control group (Fig. 1g). These results indicate that ammonia-induced upregulation of ST3GAL6 and α2,3-sialylated glycan expression occurs in astrocytes.

3.2 Astrocyte autophagy levels upregulated by ammonia

In order to clarify the autophagy changes in astrocytes induced by ammonia, we used western blotting to detect the expression of autophagy-related proteins LC3 and Beclin-1 after treatment with different concentrations of NH_4Cl. The results showed that when the concentration of NH_4Cl was 2 mmol/L, the expression of LC3 and Beclin-1 was significantly upregulated (Figs. 2a and 2b). This result suggested that the stimulation of SVGp12 cells with NH_4Cl (2 mmol/L) could increase their autophagy levels. In general, there are two possibilities for the increase in the LC3-II level. The first is that the increase in autophagy level leads to more LC3-II participating in the formation of autophagosomes. The second possibility is that the autophagy flow is inhibited, and LC3-II aggregates due to hindered degradation (Tang et al., 2022). In order to further verify that autophagy increases after NH_4Cl (2 mmol/L) stimulation, we used the lysosomal inhibitor Baf A1 to compare the changes in LC3-II between the Baf A1-treated group and the untreated group. After Baf A1 treatment, the autophagy-lysosomal pathway was inhibited, which means that the more LC3-II delivered to lysosomes for degradation (i.e., autophagy flux), the greater the expression of LC3-II observed, indicating a higher autophagy flux. Western blotting results showed that the expression level of LC3-II in the Baf A1-treated group further increased with the induction of NH_4Cl (2 mmol/L, 72 h) (Figs. 2c and 2d). This result suggested that autophagy was enhanced after induction of NH_4Cl (2 mmol/L, 72 h).

3.3 Effects of ST3GAL6 expression on autophagy levels in astrocytes

Previously, we discovered that ST3GAL6 expression was upregulated in the brain tissues of HBV transgenic mice and SVGp12 cells induced by NH_4Cl (2 mmol/L). We also found that the level of autophagy increased after NH_4Cl (2 mmol/L) induction. We speculated that the upregulated expression of ST3GAL6 induced by ammonia may be involved in the regulation of autophagy. To this end, we used two independent targeting siRNAs (siST3GAL6-1 and siST3GAL6-2) to silence ST3GAL6 in SVGp12 cells and set up a control (siCtrl). All groups were treated with NH_4Cl (2 mmol/L, 72 h). The immunoblotting result showed that silencing ST3GAL6 can inhibit the autophagy-related proteins LC3 and Beclin-1 (Figs. 3a and 3b). This result suggested that interfering with the expression of ST3GAL6 can significantly inhibit the autophagy-enhancing effect generated by NH_4Cl stimulation. There are generally two

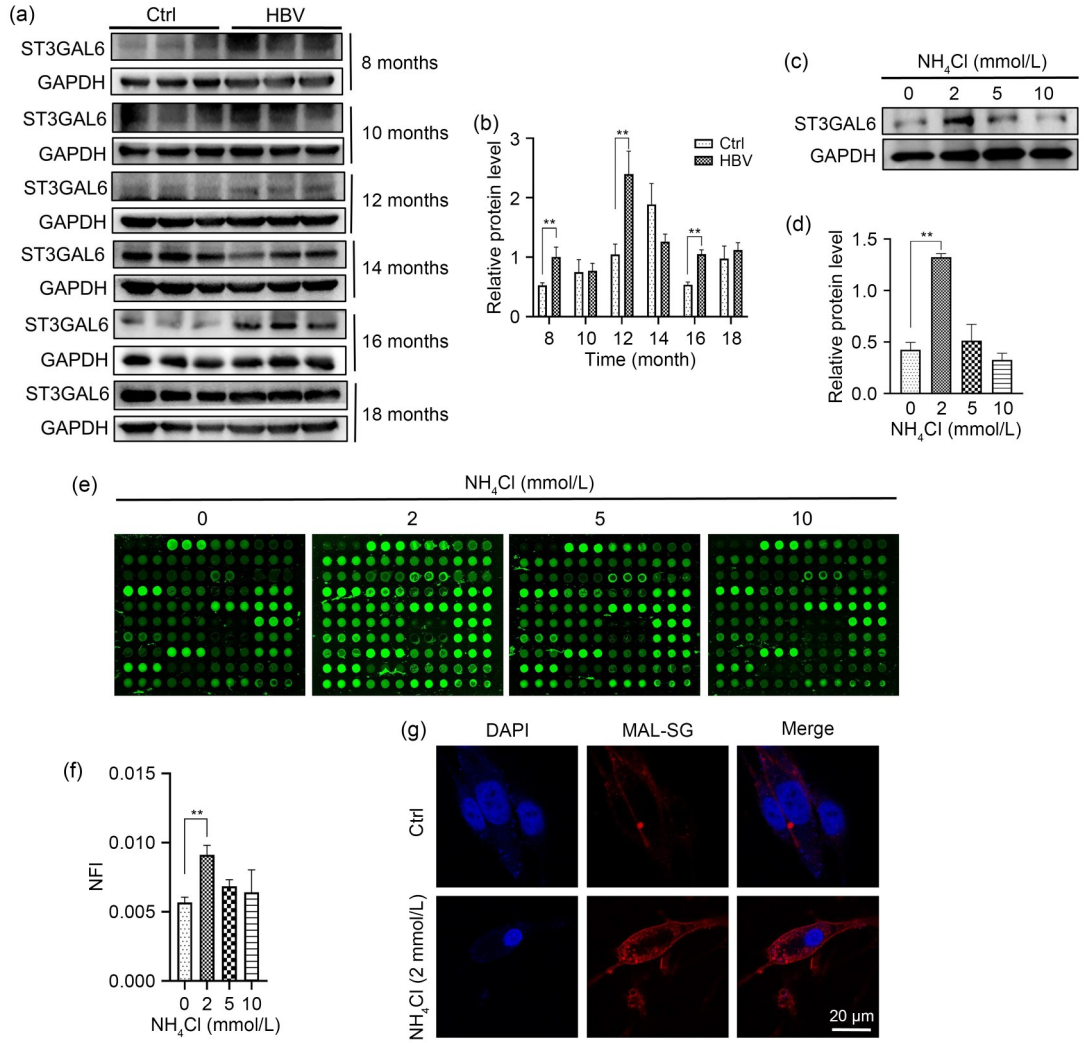

Fig. 1 Effects of ammonia on ST3 β-galactoside α2,3-sialyltransferase 6 (ST3GAL6) and α2,3-sialylated glycans in astrocytes. (a, b) ST3GAL6 protein expression levels in the brain tissues of hepatitis B virus (HBV) transgenic mice and control (Ctrl) mice at 8, 10, 12, 14, 16, and 18 months of age. Quantitative data are expressed as mean±standard deviation (SD), *n*=6. (c, d) Expression levels of ST3GAL6 protein in SVGp12 cells treated with 2, 5, and 10 mmol/L NH_4Cl, compared with the untreated group. (e, f) Cy3-labeled protein of SVGp12 cells bound to the lectin microarray and normalized fluorescence intensity (NFI) of *Maackia amurensis* lectin-II (MAL-II) in SVGp12 cells treated with 2, 5, and 10 mmol/L NH_4Cl, compared with the untreated group. Data are expressed as mean±SD of triplicate experiments. (g) The fluorescence-based lectin cytochemical demonstrated the expression of MAL-II binding α2,3-sialylated glycans (MAL-SG) in SVGp12 cells treated with NH_4Cl (2 mmol/L), compared with untreated SVGp12 cells (Ctrl). $^{**}P$<0.01. GAPDH: glyceraldehyde-3-phosphate dehydrogenase; DAPI: 4',6-diamidino-2-phenylindole.

possibilities for the downregulation of LC3-II expression. The first is that the extremely fast autophagy flow causes more LC3-II to be degraded than produced. This situation usually means that the cells are experiencing a high degree of autophagy activity. It may respond to cellular stress or other physiological conditions (Ueno and Komatsu, 2020). The second is that the initial stage of autophagy is inhibited, and the formation of autophagosomes is reduced. This situation usually indicates a reduction in autophagy activity, and the cells cannot effectively initiate the autophagy process (Kwon et al., 2022). In order to further clarify the impact of ST3GAL6 on autophagy, we used the lysosomal inhibitor Baf A1 to compare the changes in LC3-II between the Baf A1-treated and untreated groups. Western blotting results showed that, with the stimulation of NH_4Cl (2 mmol/L, 72 h), ST3GAL6 expression was silenced at the same time. There was

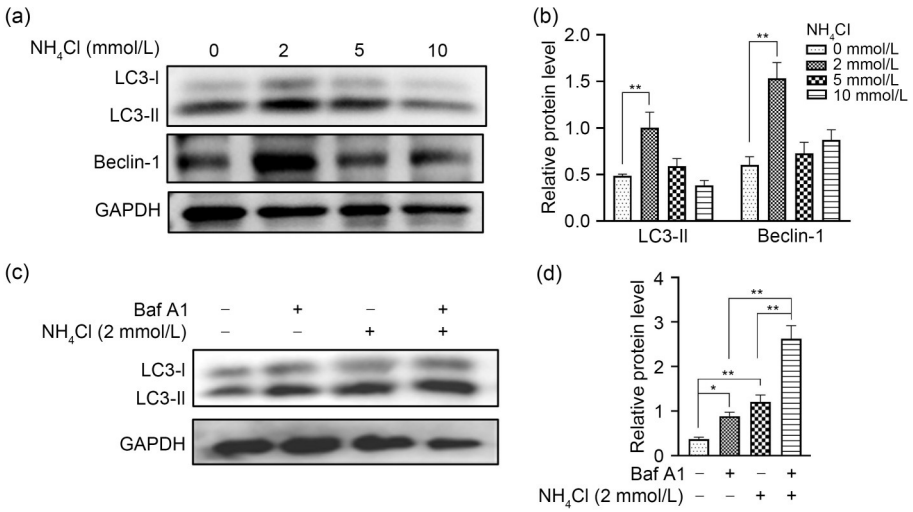

Fig. 2 Astrocyte autophagy levels upregulated by ammonia. (a, b) Microtubule-associated protein light chain 3 (LC3) and Beclin-1 protein expression levels in SVGp12 cells treated with 2, 5, and 10 mmol/L NH_4Cl, compared with the untreated group. (c, d) Expression levels of LC3 protein in SVGp12 cells treated with 2 mmol/L NH_4Cl after inhibition of the autophagosome-lysosomal pathway by bafilomycin A1 (Baf A1) (200 nmol/L). Data are expressed as mean±standard deviation (SD) of triplicate experiments. $^{*}P<0.05$, $^{**}P<0.01$. GAPDH: glyceraldehyde-3-phosphate dehydrogenase.

no significant change in the expression level of LC3 in the Baf A1-treated group or the untreated group (Figs. 3c and 3d). This result suggested that the silent expression of ST3GAL6 inhibited autophagy initiation. In addition, we looked into the level of autophagy after ST3GAL6 silencing by infecting GFP fragments produced by GFP-LC3 adenovirus (Mareninova et al., 2020). Compared with the siRNA group, the GFP fluorescent spots in the ST3GAL6 interference expression group were significantly reduced (Fig. 3e). This result further suggested that the formation of autophagosomes was inhibited after ST3GAL6 interference expression. In addition, we used lectin microarray technology to detect the expression of α2,3-sialylated glycans when silencing ST3GAL6. The results showed that the expression level of α2,3-sialylated glycans was reduced when ST3GAL6 was silenced (Figs. 3f and 3g). This result showed that the reduction in autophagy levels after ST3GAL6 silencing may be achieved by the downregulation of α2,3-sialylated glycans.

3.4 Effect of α2,3-sialylated glycans on autophagy

In order to further elucidate the relationship between α2,3-sialylated glycans and autophagy, we used MAL-II and neuraminidase to treat SVGp12 cells to block and degrade α2,3-sialylated glycans. After the cells were treated with 20 μg/mL MAL-II and 160 mU/mL neuraminidase for 72 h, and stimulated with NH_4Cl (2 mmol/L, 72 h), proteins from each group were extracted for lectin microarray analysis. The results showed that MAL-II binding α2,3-sialylated glycan (MAL-SG) was significantly reduced in the MAL-II- and neuraminidase-treated cells (Figs. 4a and 4b). This result indicated that MAL-II- and neuraminidase-treated cells play a role in blocking and degrading α2,3-sialylated glycan. At the same time, fluorescence-based lectin cytochemistry also showed that α2,3-sialylated glycan was significantly reduced after MAL-II and neuraminidase treatment of cells (Fig. 4g). We then detected the autophagy-related proteins LC3 and Beclin-1. Western blotting results showed that in the MAL-II- and neuraminidase-treated groups, the expression of LC3 and Beclin-1 was significantly reduced in a stimulus concentration-dependent manner (Figs. 4c–4f).

3.5 HSPB8-BAG3 complex upregulated by ammonia

HSPB8 is closely related to autophagy in the nervous system. Many studies have shown that HSPB8 usually forms a complex with BAG3; the HSPB8-BAG3 complex promotes the clearance of mutated or misfolded proteins by enhancing autophagy levels. Patients with HE also exhibit clinical symptoms similar to those of neurodegenerative diseases, so it is speculated that the HSPB8-BAG3 complex is also involved in the regulation of HE autophagy. In order

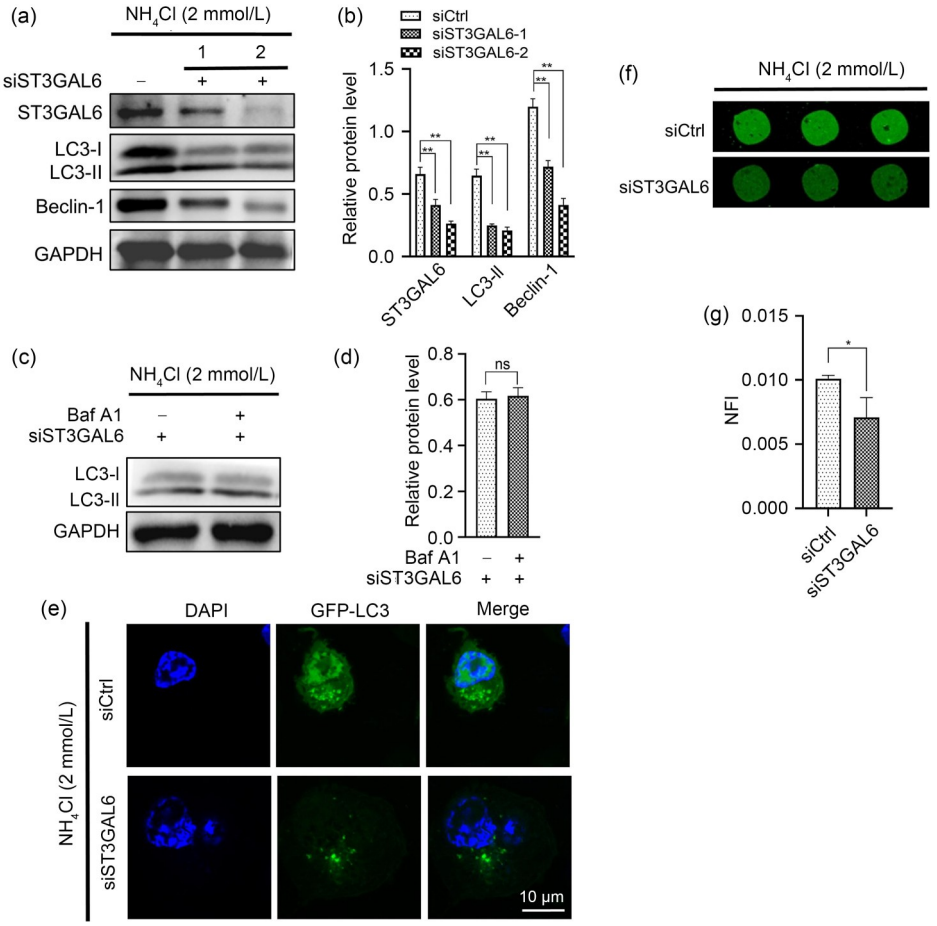

Fig. 3 Autophagy levels attenuated after silencing ST3 β-galactoside α2,3-sialyltransferase 6 (ST3GAL6) expression in astrocytes. (a, b) Protein expression levels of microtubule-associated protein light chain 3 (LC3) and Beclin-1 after ST3GAL6 silencing (two targets). (c, d) LC3 protein expression levels after ST3GAL6 silencing in the presence of bafilomycin A1 (Baf A1; 200 nmol/L), an inhibitor of the autophagosome-lysosomal pathway. (e) Infection of SVGp12 cells with green fluorescent protein (GFP)-LC3 adenovirus, treated with NH_4Cl (2 mmol/L), and comparison of changes in GFP-LC3 green fluorescent spots between the ST3GAL6 interference expression group and the noninterference expression group. (f, g) Cy3-labeled protein of SVGp12 cells bound to the lectin microarray and normalized fluorescence intensity (NFI) of lectin *Maackia amurensis* lectin-II (MAL-II) (Siaα2-3Gal/GalNAc binder) following ST3GAL6 silencing. Data are expressed as mean±standard deviation (SD) of triplicate experiments. $^{*}P<0.05$, $^{**}P<0.01$; ns, not significant. si: small interfering RNA; Ctrl: control; GAPDH: glyceraldehyde-3-phosphate dehydrogenase; DAPI: 4',6-diamidino-2-phenylindole (Note: for interpretation of the references to color in this figure legend, the reader is referred to the web version of this article).

to verify this speculation, we first detected the expression in the brain tissues of HBV transgenic mice and negative control mice. Western blotting results showed that the expression of HSPB8 was significantly upregulated at 8, 12, 16, and 18 months of age (Figs. 5c and 5e); the expression of BAG3 was significantly upregulated at 8, 12, 16, and 18 months of age (Figs. 5d and 5e). At the same time, astrocytes were analyzed using immunoblotting after being treated with 2, 5, or 10 mmol/L NH_4Cl for 72 h; we observed that the expression of HSPB8 and BAG3 was significantly upregulated when stimulated by NH_4Cl (2 mmol/L) (Figs. 5a and 5b). These results suggest that HSPB8-BAG3 is closely related to HE.

3.6 Autophagy modulated by ST3GAL6 via HSPB8-BAG3 complex

We have already made it clear that the silent expression of ST3GAL6 mainly affects the initial stage of autophagy. The expression of ST3GAL6 and the HSPB8-BAG3 complex is upregulated under ammonia induction. Whether ST3GAL6 regulates autophagy

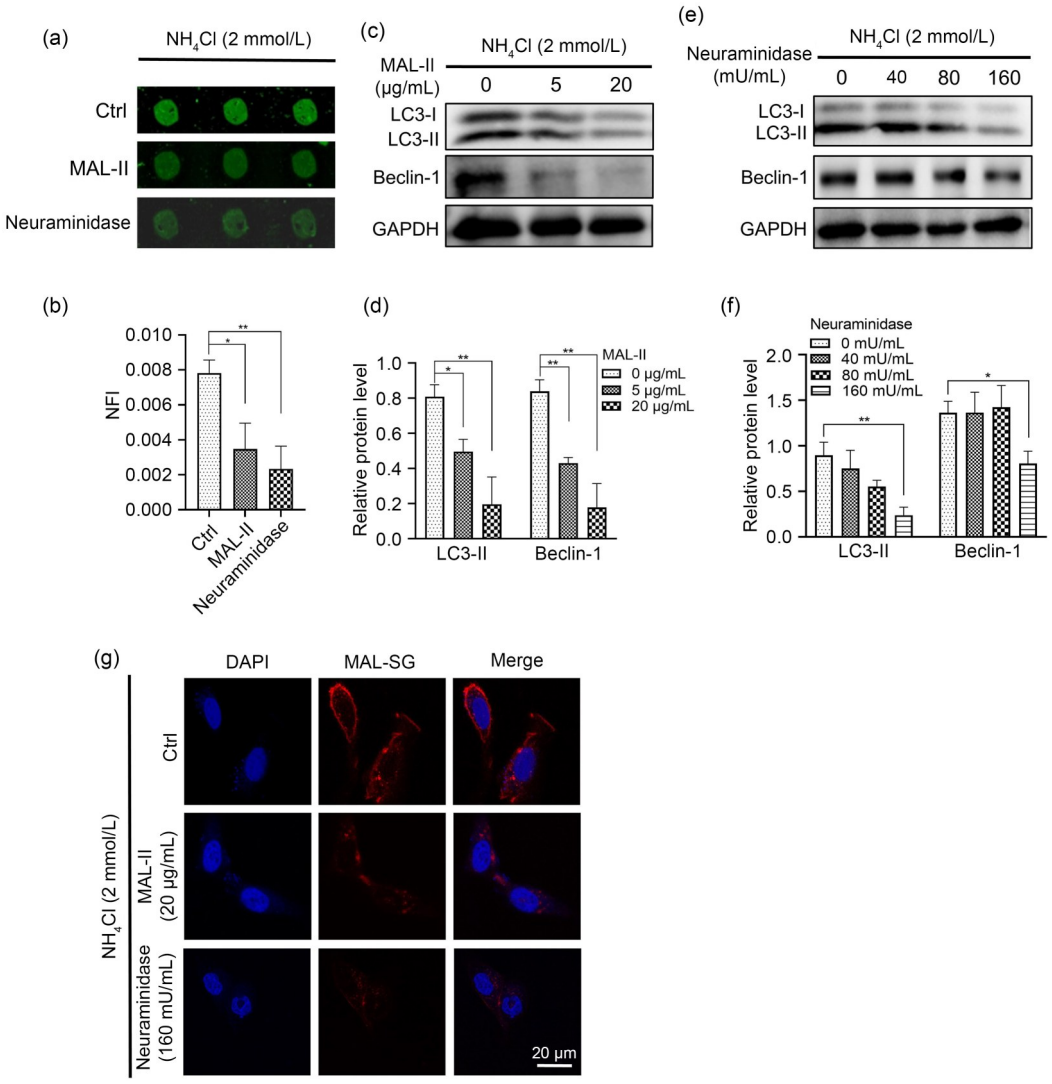

Fig. 4 Effect of α2,3-sialylated glycans on autophagy. (a, b) Cy3-labeled protein of SVGp12 cells bound to the lectin microarray and normalized fluorescence intensity (NFI) of *Maackia amurensis* lectin-II (MAL-II) (Siaα2-3Gal/GalNAc binder) following the treatment of SVGp12 cells with MAL-II (20 μg/mL) and neuraminidase (160 mU/mL). (c, d) The microtubule-associated protein light chain 3 (LC3) and Beclin-1 protein expression levels in SVGp12 cells treated with MAL-II (5 and 20 μg/mL). (e, f) LC3 and Beclin-1 protein expression levels in SVGp12 cells treated with neuraminidase (40, 80, and 160 mU/mL). (g) The fluorescence-based lectin cytochemical demonstrated the expression of MAL-II binding α2,3-sialylated glycans (MAL-SG) in SVGp12 cells treated with MAL-II (20 μg/mL) and neuraminidase (160 mU/mL), compared with untreated SVGp12 cells (Ctrl). Data are expressed as mean±standard deviation (SD) of triplicate experiments. $^{*}P<0.05$, $^{**}P<0.01$. Ctrl: control; GAPDH: glyceraldehyde-3-phosphate dehydrogenase; DAPI: 4',6-diamidino-2-phenylindole.

through the HSPB8-BAG3 complex is worthy of attention. To further elucidate the relationship between ST3GAL6 and the HSPB8-BAG3 complex in autophagy regulation, we first examined the effect of ST3GAL6 silencing on the HSPB8-BAG3 complex in the presence of NH_4Cl (2 mmol/L) stimulation. Western blotting showed that silencing ST3GAL6 reduced the expression level of the HSPB8-BAG3 complex (Figs. 6a and 6b). Interestingly, we found that the expression of the HSPB8-BAG3 complex was also reduced after cells were treated with MAL-II and neuraminidase (Figs. 6c–6f). This result suggested that ST3GAL6 affected HSPB8-BAG3 expression through α2,3-sialylated glycan. In addition, we overexpressed HSPB8, and western blotting results showed that, compared with the vector group, the expression of autophagy-related proteins LC3-II and Beclin-1 was upregulated when HSPB8 was overexpressed, indicating

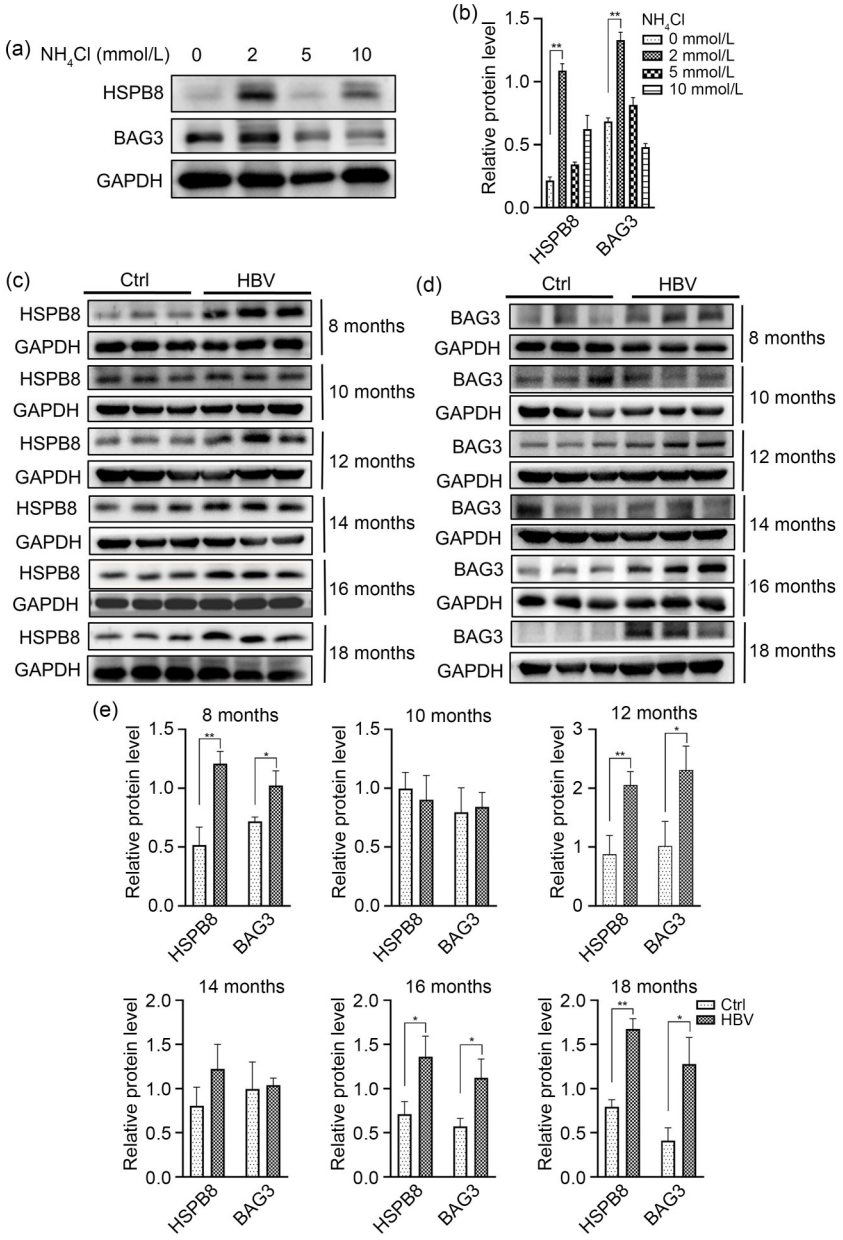

Fig. 5 Heat shock protein β8 (HSPB8)-Bcl2-associated athanogene 3 (BAG3) complex upregulated by ammonia. (a, b) HSPB8 and BAG3 protein expression levels in SVGp12 cells treated with 2, 5, and 10 mmol/L NH_4Cl. (c–e) HSPB8 and BAG3 protein expression levels in the brain tissues of hepatitis B virus (HBV) transgenic mice and control (Ctrl) mice at 8, 10, 12, 14, 16, and 18 months of age. Data are expressed as mean±standard deviation (SD), n=6. $^{*}P$<0.05, $^{**}P$<0.01. GAPDH: glyceraldehyde-3-phosphate dehydrogenase.

that the level of autophagy was enhanced (Figs. 6g and 6h). At the same time, we found that BAG3 expression was also upregulated (Figs. 6g and 6h). Based on the above findings, we speculated whether HSPB8 overexpression could restore the reduced autophagy level caused by ST3GAL6. We overexpressed HSPB8 while silencing ST3GAL6, and western blotting results showed that, compared with the ST3GAL6 silencing group alone, the ST3GAL6 interference expression and HSPB8 overexpression group resulted in the upregulation of autophagy-related protein LC3-II, which partially reversed the reduced autophagy levels caused by silencing ST3GAL6 expression (Figs. 6i and 6j). Taken together, the above results indicate that ST3GAL6 affects the level of autophagy by regulating the HSPB8-BAG3 complex (Fig. 6k).

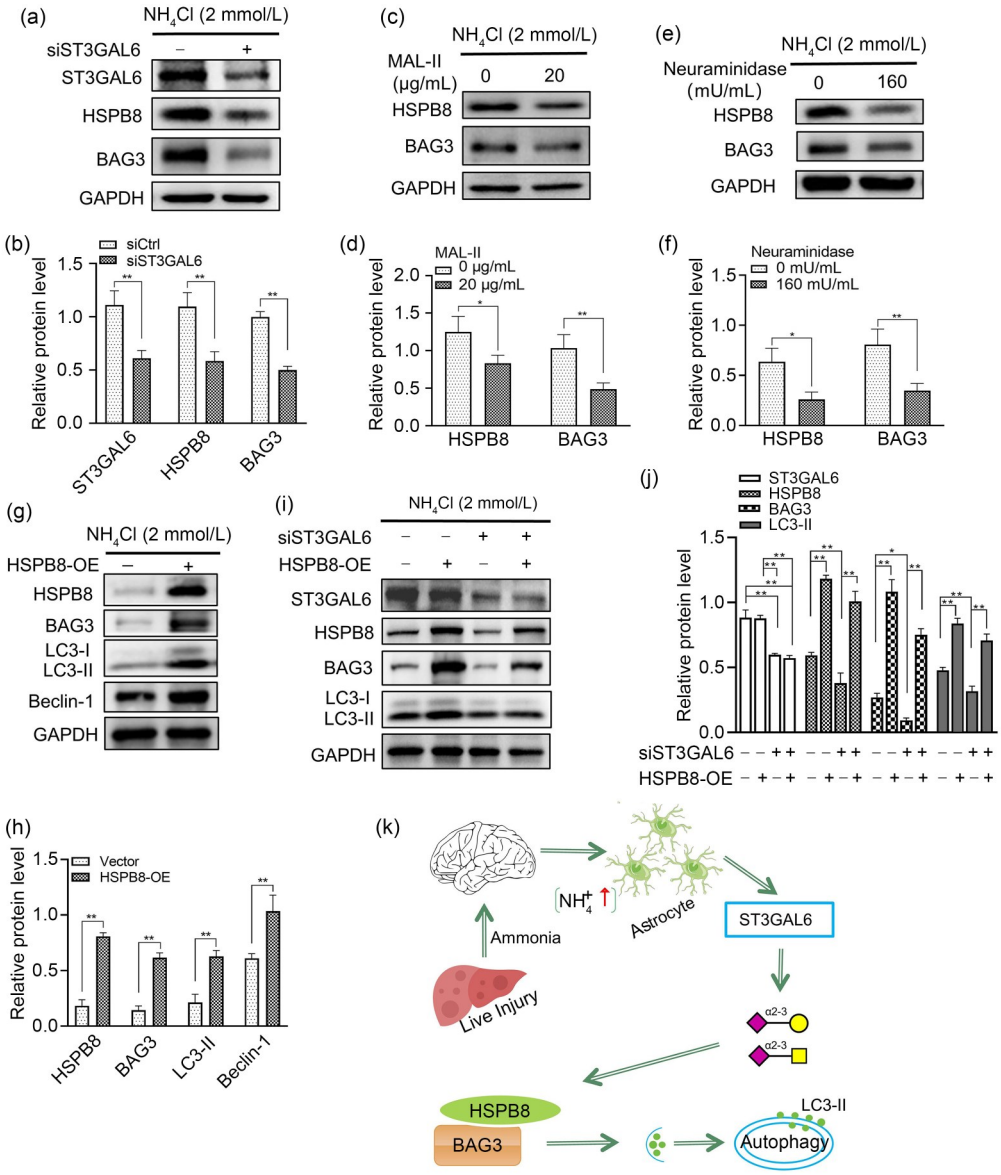

Fig. 6 Autophagy modulated by ST3 β-galactoside α2,3-sialyltransferase 6 (ST3GAL6) via heat shock protein β8 (HSPB8)-Bcl2-associated athanogene 3 (BAG3) complex. (a, b) Expression levels of HSPB8 and BAG3 proteins after ST3GAL6 silencing. (c, d) HSPB8 and BAG3 protein expression levels in SVGp12 cells treated with *Maackia amurensis* lectin-II (MAL-II) (20 μg/mL). (e, f) HSPB8 and BAG3 protein expression levels in SVGp12 cells treated with neuraminidase (160 mU/mL). (g, h) Protein expression levels of BAG3, microtubule-associated protein light chain 3 (LC3), and Beclin-1 after HSPB8 overexpression (OE). (i, j) Overexpression of HSPB8 partially reverses the inhibitory effect of ST3GAL6 silencing on autophagy. (k) Schematic representation of ST3GAL6 regulating autophagy and related mechanisms in hepatic encephalopathy (HE). Data are expressed as mean±standard deviation (SD) of triplicate experiments. $^{*}P<0.05$, $^{**}P<0.01$. si: small interfering RNA; Ctrl: control; GAPDH: glyceraldehyde-3-phosphate dehydrogenase.

4 Discussion

Sialylation is a significant type of glycosylation in the brain, and abnormal sialylation is closely associated with neurological diseases (Li and Ding, 2019; Siddiqui et al., 2019; Yang et al., 2021). HE is a common complication of end-stage liver disease, leading to irreversible and persistent neurological complications. In our study, we observed an upregulation of ST3GAL6 expression in the brain tissue of HBV transgenic mice at 8, 12, and 16 months. Interestingly, we also noticed an increase in both ST3GAL6 and α2,3-sialylated

glycans in astrocytes treated with NH_4Cl. The results suggested a close relationship between ammonia induction and the upregulated expression of ST3GAL6 and α2, 3-sialylated glycans. It is observed that the complex pathological processes involved in HE, such as immune response, neuroinflammation, and axon regeneration, are closely related to sialylation. The upregulation of ST3GAL6 and α2,3-sialylated glycans induced by ammonia may impact the development of HE by influencing these pathological processes. Furthermore, there have been reports of *ST3GAL6* mutations in the neurodegenerative disease ALS, indicating a potential connection between ST3GAL6 and neurological diseases (Togawa et al., 2019). However, the exact roles of ST3GAL6 in disease and its regulatory mechanisms remain unknown. Furthermore, we recognize that modulating pathways that mitigate oxidative stress, inflammation, and metabolic dysfunctions can ameliorate liver injury (Huang et al., 2023). Protein kinase B (AKT) and protein 38 (p38) mitogen-activated protein kinase (MAPK)/nuclear factor-κB (NF-κB) are pivotal in regulating these pathways and have a profound connection to autophagy (Bao et al., 2023; Zhang et al., 2023). Nevertheless, the regulatory nexus between ST3GAL6 and these molecules is sparsely documented. This gap underscores the importance of our future research in deciphering the intricate interplay among oxidative stress, inflammatory responses, and autophagy with respect to ST3GAL6.

Autophagy is closely related to neurodegenerative diseases; many studies have shown that these diseases often involve the accumulation and aggregation of abnormal proteins, and autophagy plays a neuroprotective role by recognizing and degrading these abnormal proteins (Park et al., 2020; Barmaki et al., 2023). The relationship between ammonia and autophagy is complex; some studies have pointed out that ammonia has a dual effect on autophagy. An increase in concentration below 10 mmol/L tends to enhance autophagy, while a higher concentration above 20 mmol/L will damage the autophagy pathway (Soria and Brunetti-Pierri, 2019; Shen et al., 2020). Here, our results show that the level of autophagy is significantly increased in astrocytes treated with a lower concentration of NH_4Cl (2 mmol/L), which is consistent with other reports (Lu et al., 2019). Silencing ST3GAL6 in astrocytes resulted in reduced levels of α2,3-sialylated glycans and autophagy. The initial stage of autophagy was found to be inhibited when ST3GAL6 was silenced, as demonstrated by the use of the lysosomal inhibitor Baf A1. Additionally, blocking and degrading α2,3-sialylated glycans also led to a reduction in autophagy. These findings suggest that ST3GAL6 regulates autophagy by affecting α2,3-sialylated glycans. Previous studies have indicated that ST3GAL6 promotes the proliferation and invasion of hepatocellular carcinoma and colon cancer cells through the phosphoinositide 3-kinase (PI3K)/AKT signaling pathway (Sun et al., 2017; Hu et al., 2019). It is worth noting that the PI3K/AKT pathway is closely associated with autophagy. Activation of the PI3K/AKT pathway activates mechanistic target of rapamycin complex 1 (mTORC1); after activation, mTORC1 further regulates downstream molecules to inhibit the initiation of autophagy (Dai et al., 2021; Xu et al., 2021). Moreover, the PI3K/AKT pathway can directly impact autophagy-related proteins, such as phosphorylating the autophagy-related gene transcription factor forkhead box O (FOXO) protein family, which affects the autophagy process (Abdullah et al., 2021). Although our study did not investigate the regulatory relationship between ST3GAL6 and the PI3K/AKT pathway, these reports suggest a potential mechanism for ST3GAL6 regulation of autophagy and provide valuable insights for future research.

There have been limited studies on the direct substrates of ST3GAL6. However, a recent study caught our attention, as it demonstrated that knocking out *ST3GAL6* in HeLa cells significantly reduced the α2,3-sialylation level of the epidermal growth factor receptor (EGFR). On the other hand, overexpression of ST3GAL6 successfully restored total α2,3-sialylation levels and α2,3-sialylation of EGFR (Qi et al., 2020). It is worth noting that the relationship between EGFR and autophagy has been extensively investigated. In brief, EGFR primarily regulates autophagy through three signaling pathways: EGFR/PI3K/AKT/mechanistic target of rapamycin (mTOR), EGFR/MAPK1/3, and EGFR/Janus kinase 2 (JAK2)/signal transducer and activator of transcription 3 (STAT3) (Li et al., 2017; Vishwakarma et al., 2023). As we discussed earlier, ST3GAL6 regulates the PI3K/AKT pathway, and EGFR, being a substrate of ST3GAL6, also acts as an upstream regulator of the PI3K/AKT pathway. Therefore, we can infer that EGFR α2,3-sialylation plays a crucial role in the regulation of the EGFR/PI3K/AKT pathway, which further elucidates the regulatory effect of ST3GAL6 on autophagy.

In neurodegenerative diseases, the HSPB8-BAG3 complex is involved in the regulation of autophagy (Lin et al., 2022; Chierichetti et al., 2023), but it is still unknown whether HSPB8-BAG3 is involved in the regulation of autophagy in HE. Our data show that, in the brain tissue of HBV transgenic mice, the expression of HSPB8 and BAG3 was significantly upregulated at ages of 8, 12, 16, and 18 months. In astrocytes treated with NH_4Cl (2 mmol/L), upregulation of HSPB8 and BAG3 was also observed, consistent with the relevant report in neurodegenerative diseases (Seidel et al., 2012). Furthermore, we observed that silencing ST3GAL6 led to a decrease in HSPB8 and BAG3 expression, resulting in reduced autophagy levels. However, when HSPB8 was overexpressed, it partially restored the autophagy reduction caused by ST3GAL6 silencing. This finding suggests that ST3GAL6 regulates autophagy through the HSPB8-BAG3 complex. Notably, blocking and degrading α2,3-sialylated glycans in SVGp12 cells also led to the downregulation of HSPB8 and BAG3 expression. This further supports the idea that ST3GAL6 silencing affects the expression of α2,3-sialylated glycans and reduces autophagosome formation by downregulating HSPB8 and BAG3. It is important to mention that, although this study has shed light on the regulatory effect of ST3GAL6 on HSPB8-BAG3, the specific sialylated protein that ST3GAL6 directly targets in the regulatory pathway remains uncertain. Therefore, further investigation is warranted to elucidate the specific mechanism.

5 Conclusions

In summary, ST3GAL6 may act as a mediator of the upregulation of α2,3-sialylated glycans during hyperammonemia, thereby affecting the level of autophagy by regulating the HSPB8-BAG3 complex. Autophagy plays a crucial role in preventing and intervening in neurological damage. Therefore, we believe that enhancing autophagy may improve the disease trajectory of HE. Our study demonstrates the complex interactions between ST3GAL6 and α2,3-sialylated glycans and their roles in HE. Notably, our study can coordinate autophagy by manipulating ST3GAL6, providing a new perspective for intervening in HE.

Data availability statement

The data presented in this study are available from the corresponding author upon reasonable request.

Acknowledgments

This work was supported by the National Natural Science Foundation of China (No. 82370592), the Discipline Construction Project of the Health System in Pudong New Area (No. PWZbr2022-15), and the Pudong New Area Special Fund for Livelihood Research Project of Science and Technology Development Fund (No. PKJ2021-Y12), China.

Author contributions

Xiaocheng LI, Yonghong GUO, Huijie BIAN, and Zheng LI conceived and designed experiments. Xiaocheng LI, Yaqing XIAO, Pengfei LI, and Yayun ZHU designed and performed the experiments. Xiaocheng LI and Pengfei LI designed and performed the data acquisition and analysis. Yonghong GUO helped with critical advice and discussion. Xiaocheng LI, Yonghong GUO, Huijie BIAN, and Zheng LI prepared the manuscript. All authors have read and approved the final manuscript, and therefore, have full access to all the data in the study and take responsibility for the integrity and security of the data.

Compliance with ethics guidelines

Xiaocheng LI, Yaqing XIAO, Pengfei LI, Yayun ZHU, Yonghong GUO, Huijie BIAN, and Zheng LI declare no conflict of interest.

The ethical approval for the animal experiment was obtained from the Ethics Committee and Institutional Review Committee of the National Center for Translational Science of Molecular Medicine of Fourth Military Medical University, Xi'an, China (No. 2022-NTSCMM-ID006).

References

Abdullah ML, Al-Shabanah O, Hassan ZK, et al., 2021. Eugenol-induced autophagy and apoptosis in breast cancer cells via PI3K/AKT/FOXO3a pathway inhibition. *Int J Mol Sci*, 22(17):9243. https://doi.org/10.3390/ijms22179243

Bao T, Karim N, Ke HH, et al., 2023. Polysaccharide isolated from wax apple suppresses ethyl carbamate-induced oxidative damage in human hepatocytes. *J Zhejiang Univ-Sci B (Biomed & Biotechnol)*, 24(7):574-586. https://doi.org/10.1631/jzus.B2200629

Barmaki H, Nourazarian A, Khaki-Khatibi F, 2023. Proteostasis and neurodegeneration: a closer look at autophagy in Alzheimer's disease. *Front Aging Neurosci*, 15:1281338. https://doi.org/10.3389/fnagi.2023.1281338

Bowles WHD, Gloster TM, 2021. Sialidase and sialyltransferase inhibitors: targeting pathogenicity and disease. *Front Mol Biosci*, 8:705133. https://doi.org/10.3389/fmolb.2021.705133

Chierichetti M, Cerretani M, Ciammaichella A, et al., 2023.

Identification of HSPB8 modulators counteracting misfolded protein accumulation in neurodegenerative diseases. *Life Sci*, 322:121323. https://doi.org/10.1016/j.lfs.2022.121323

Dai H, Hu WJ, Zhang LY, et al., 2021. FGF21 facilitates autophagy in prostate cancer cells by inhibiting the PI3K–Akt–mTOR signaling pathway. *Cell Death Dis*, 12(4):303. https://doi.org/10.1038/S41419-021-03588-W

Dalangood S, Zhu Z, Ma ZH, et al., 2020. Identification of glycogene-type and validation of ST3GAL6 as a biomarker predicts clinical outcome and cancer cell invasion in urinary bladder cancer. *Theranostics*, 10(22):10078-10091. https://doi.org/10.7150/thno.48711

Fallahzadeh MA, Rahimi RS, 2022. Hepatic encephalopathy: current and emerging treatment modalities. *Clin Gastroenterol Hepatol*, 20(S8):S9-S19. https://doi.org/10.1016/j.cgh.2022.04.034

Filippone A, Esposito E, Mannino D, et al., 2022. The contribution of altered neuronal autophagy to neurodegeneration. *Pharmacol Ther*, 238:108178. https://doi.org/10.1016/j.pharmthera.2022.108178

Friedman J, 2011. Why is the nervous system vulnerable to oxidative stress? *In*: Gadoth N, Göbel HH (Eds.), Oxidative Stress and Free Radical Damage in Neurology. Springer, Totowa, p.19-27. https://doi.org/10.1007/978-1-60327-514-9_2

Hu JL, Shan YJ, Ma J, et al., 2019. LncRNA ST3Gal6-AS1/ST3Gal6 axis mediates colorectal cancer progression by regulating α-2,3 sialylation *via* PI3K/Akt signaling. *Int J Cancer*, 145(2):450-460. https://doi.org/10.1002/ijc.32103

Huang JJ, Bai YM, Xie WT, et al., 2023. *Lycium barbarum* polysaccharides ameliorate canine acute liver injury by reducing oxidative stress, protecting mitochondrial function, and regulating metabolic pathways. *J Zhejiang Univ-Sci B (Biomed & Biotechnol)*, 24(2):157-171. https://doi.org/10.1631/jzus.B2200213

Huang JM, Huang JM, Zhang GN, 2022. Insights into the role of sialylation in cancer metastasis, immunity, and therapeutic opportunity. *Cancers*, 14(23):5840. https://doi.org/10.3390/cancers14235840

Kim CH, 2020. Sialyltransferase, sialylation, and sulfoylation. *In*: Kim CH (Ed.), Ganglioside Biochemistry. Springer, Singapore, p.35-53. https://doi.org/10.1007/978-981-15-5815-3_3

Kwon Y, Haam CE, Byeon S, et al., 2022. Effects of 3-methyladenine, an autophagy inhibitor, on the elevated blood pressure and arterial dysfunction of angiotensin II-induced hypertensive mice. *Biomed Pharmacother*, 154:113588. https://doi.org/10.1016/j.biopha.2022.113588

Lawrence JM, Schardien K, Wigdahl B, et al., 2023. Roles of neuropathology-associated reactive astrocytes: a systematic review. *Acta Neuropathol Commun*, 11:42. https://doi.org/10.1186/s40478-023-01526-9

Li FJ, Ding JJ, 2019. Sialylation is involved in cell fate decision during development, reprogramming and cancer progression. *Protein Cell*, 10(8):550-565. https://doi.org/10.1007/s13238-018-0597-5

Li HS, You LK, Xie JS, et al., 2017. The roles of subcellularly located EGFR in autophagy. *Cell Signal*, 35:223-230. https://doi.org/10.1016/j.cellsig.2017.04.012

Li JX, Long YM, Sun JY, et al., 2022. Comprehensive landscape of the ST3GAL family reveals the significance of ST3GAL6-AS1/ST3GAL6 axis on EGFR signaling in lung adenocarcinoma cell invasion. *Front Cell Dev Biol*, 10:931132. https://doi.org/10.3389/fcell.2022.931132

Lin H, Koren SA, Cvetojevic G, et al., 2022. The role of BAG3 in health and disease: a "Magic BAG of Tricks". *J Cell Biochem*, 123(1):4-21. https://doi.org/10.1002/jcb.29952

Lu KH, Zimmermann M, Görg B, et al., 2019. Hepatic encephalopathy is linked to alterations of autophagic flux in astrocytes. *eBioMedicine*, 48:539-553. https://doi.org/10.1016/j.ebiom.2019.09.058

Mareninova OA, Jia WZ, Gretler SR, et al., 2020. Transgenic expression of GFP-LC3 perturbs autophagy in exocrine pancreas and acute pancreatitis responses in mice. *Autophagy*, 16(11):2084-2097. https://doi.org/10.1080/15548627.2020.1715047

Ochoa-Sanchez R, Tamnanloo F, Rose CF, 2021. Hepatic encephalopathy: from metabolic to neurodegenerative. *Neurochem Res*, 46(10):2612-2625. https://doi.org/10.1007/s11064-021-03372-4

Park H, Kang JH, Lee S, 2020. Autophagy in neurodegenerative diseases: a hunter for aggregates. *Int J Mol Sci*, 21(9):3369. https://doi.org/10.3390/ijms21093369

Peker N, Gozuacik D, 2020. Autophagy as a cellular stress response mechanism in the nervous system. *J Mol Biol*, 432(8):2560-2588. https://doi.org/10.1016/j.jmb.2020.01.017

Qi F, Isaji T, Duan CW, et al., 2020. ST3GAL3, ST3GAL4, and ST3GAL6 differ in their regulation of biological functions via the specificities for the α2,3-sialylation of target proteins. *FASEB J*, 34(1):881-897. https://doi.org/10.1096/fj.201901793R

Rose CF, Amodio P, Bajaj JS, et al., 2020. Hepatic encephalopathy: novel insights into classification, pathophysiology and therapy. *J Hepatol*, 73(6):1526-1547. https://doi.org/10.1016/j.jhep.2020.07.013

Seidel K, Vinet J, den Dunnen WFA, et al., 2012. The HSPB8-BAG3 chaperone complex is upregulated in astrocytes in the human brain affected by protein aggregation diseases. *Neuropathol Appl Neurobiol*, 38(1):39-53. https://doi.org/10.1111/j.1365-2990.2011.01198.x

Sepehrinezhad A, Zarifkar A, Namvar G, et al., 2020. Astrocyte swelling in hepatic encephalopathy: molecular perspective of cytotoxic edema. *Metab Brain Dis*, 35(4):559-578. https://doi.org/10.1007/s11011-020-00549-8

Shen Y, Malik SA, Amir M, et al., 2020. Decreased hepatocyte autophagy leads to synergistic IL-1β and TNF mouse liver injury and inflammation. *Hepatology*, 72(2):595-608.

https://doi.org/10.1002/hep.31209

Siddiqui SS, Matar R, Merheb M, et al., 2019. Siglecs in brain function and neurological disorders. *Cells*, 8(10):1125. https://doi.org/10.3390/cells8101125

Soria LR, Brunetti-Pierri N, 2019. Ammonia and autophagy: an emerging relationship with implications for disorders with hyperammonemia. *J Inherit Metab Dis*, 42(6):1097-1104. https://doi.org/10.1002/jimd.12061

Sun MM, Zhao XZ, Liang LL, et al., 2017. Sialyltransferase ST3GAL6 mediates the effect of microRNA-26a on cell growth, migration, and invasion in hepatocellular carcinoma through the protein kinase B/mammalian target of rapamycin pathway. *Cancer Sci*, 108(2):267-276. https://doi.org/10.1111/cas.13128

Tang HY, Huang HY, Wang D, et al., 2022. TFEB ameliorates autophagy flux disturbance induced by PBDE-47 via up-regulating autophagy-lysosome fusion. *J Hazard Mater*, 430:128483. https://doi.org/10.1016/j.jhazmat.2022.128483

Togawa J, Ohi T, Yuan JH, et al., 2019. Atypical familial amyotrophic lateral sclerosis with slowly progressing lower extremities-predominant late-onset muscular weakness and atrophy. *Intern Med*, 58(13):1851-1858. https://doi.org/10.2169/internalmedicine.2222-18

Ueno T, Komatsu M, 2020. Monitoring autophagy flux and activity: principles and applications. *BioEssays*, 42(11):2000122. https://doi.org/10.1002/bies.202000122

Vishwakarma J, Gupta K, Mishra J, et al., 2023. Hypothyroidism induces motor deficit via altered cerebellar HB-EGF/EGFR and autophagy. *J Endocrinol*, 257(1):e220338. https://doi.org/10.1530/JOE-22-0338

Xu K, He YZ, Moqbel SAA, et al., 2021. SIRT3 ameliorates osteoarthritis via regulating chondrocyte autophagy and apoptosis through the PI3K/Akt/mTOR pathway. *Int J Biol Macromol*, 175:351-360. https://doi.org/10.1016/j.ijbiomac.2021.02.029

Yang KK, Yang ZF, Chen XF, et al., 2021. The significance of sialylation on the pathogenesis of Alzheimer's disease. *Brain Res Bull*, 173:116-123. https://doi.org/10.1016/j.brainresbull.2021.05.009

Zhang X, Dong Z, Fan H, et al., 2023. Scutellarin prevents acute alcohol-induced liver injury via inhibiting oxidative stress by regulating the Nrf2/HO-1 pathway and inhibiting inflammation by regulating the AKT, p38 MAPK/NF-κB pathways. *J Zhejiang Univ-Sci B (Biomed & Biotechnol)*, 24(7):617-631. https://doi.org/10.1631/jzus.B2200612

Supplementary information

Table S1; Fig. S1